

# Realizing microrheological response of configurable viscoelastic media with a dynamic optical trap

Sanatan Halder <sup>1,\*</sup> and Manas Khan <sup>1,†</sup>

<sup>1</sup>*Department of Physics, Indian Institute of Technology Kanpur, Kanpur - 208016, India*

The local viscoelastic (VE) environment governs the motion of an embedded microsphere and consequently, pertinent dynamical phenomena. However, studying such phenomena with varying VE properties remains challenging for various reasons, including the strong coupling among the VE parameters and their dependence on experimental conditions, such as temperature. Here, we demonstrate the experimental realization of configurable VE media with broad variations, wherein the VE properties can be systematically and independently tuned, employing a dynamic optical trap. Specifically, the dynamics of a particle in a slowly diffusing optical trap provides the linear microrheological response of single-relaxation VE fluids, namely Jeffreys or Maxwell-Voigt (MV) fluids, where the trap strength and its diffusion coefficient regulate the elastic response and the low-frequency viscosity, respectively. We validate this approach by comparing the experimentally observed dynamics of the trapped bead with those of a probe particle in real single-relaxation complex fluids, analytical predictions, and simulation results following harmonically bound Brownian particle with long-time diffusion model describing MV fluids. We extend the applicability of this scheme for realizing the microrheological response of double-relaxation VE media by incorporating appropriately correlated noise in the trap trajectory, signifying its validity for any linear VE media with multiple relaxations. Our scheme can be further extended to realize probe particle dynamics in an active VE environment, e.g., an entangled network of active polymers, by translating the trap along an active Brownian trajectory. Therefore, our scheme enables systematic microrheological studies in VE regimes that are otherwise challenging to realize or not readily accessible with real materials.

Keywords: Configurable viscoelasticity, Dynamic optical trap, Linear microrheological response, Maxwell-Voigt fluid, Active viscoelastic environments, Microrheology

**Introduction** – Complex fluids, including wormlike micelles [1–6], emulsions [7], entangled polymer solutions [8–14], biopolymer networks [15–17], and active polymers [18–22], exhibit viscoelastic (VE) properties that govern microscale transport and relaxation dynamics [23]. The frequency-dependent shear moduli of these materials profoundly influence the motion of embedded colloidal probes [24]. This connection between probe dynamics and material properties offers a direct window into the VE response of complex fluids. The resulting framework is used in microrheology, where the translational and orientational thermal motion of probe particles embedded in complex fluids reveals the VE properties of their environment through the generalized Stokes-Einstein relation (GSER) [7, 10, 12, 14, 23–29]. Constitutive models representing linear VE responses greatly aid in the understanding and interpretation of probe dynamics. Many studies employ the Jeffreys fluid model, which describes single-relaxation complex fluids with a Voigt element, constituted by a spring and dashpot in parallel, and another dashpot in series [30, 31]. The Voigt element is the simplest rheological model for an elastoviscous medium, capturing elastic recovery alongside viscous dissipation. The Maxwell-Voigt (MV) fluid extends this framework by connecting a Maxwell element with a Voigt element in series, where the Maxwell element is represented by a spring and dashpot in series, with a shared spring constant  $k$ , providing an enhanced description of materials with pronounced elastic plateaus [32–36].

Knowledge of the local microrheological response of the medium is crucial for comprehending complex transport phe-

nomena across mesoscopic length scales, ranging from intracellular transport to microorganism motility in the mucus [37–40]. However, studying probe dynamics in real complex fluids in the desired VE regimes or in specific settings presents significant experimental challenges. The VE properties of these systems depend sensitively on temperature, concentration, and sample age [2, 8, 41], whereas the microrheological response varies with active forcing [42], particle size [13, 43], and surface chemistry [44]. Moreover, material parameters such as relaxation time, viscosity, and elastic modulus are inherently coupled, making it impossible to vary a single parameter independently for systematic studies. These limitations underscore the necessity of developing experimental approaches in which the VE environment can be precisely configured and systematically tuned.

Here, we demonstrate an experimental scheme using a dynamic optical trap to obtain the linear microrheological response of a configurable VE medium. Drawing motivation from the harmonically bound Brownian particle (HBBP) with long-time diffusion model [45], we steer an optical trap, which harmonically confines a Brownian probe particle, along an appropriate trajectory to realize the desired relaxation behavior of the emergent VE environment. This approach enables us to fully configure the relaxation dynamics of the medium, manifesting single-relaxation, double-relaxation, or even active relaxation, which is observed in far-from-equilibrium entangled networks of active polymers. While moving the optical trap along a free diffusive trajectory generates a single relaxation, as observed in the MV or Jeffrey fluid, trap trajectories with correlated translational noise give rise to another elastic confinement regime at a longer time, manifested as a second plateau, with an eventual second relaxation. Active relaxation is observed when the trap is moved following the trajectory

\* sanatanh@iitk.ac.in

† mkhan@iitk.ac.in

of an active Brownian particle. Furthermore, this scheme provides independent tunability of various VE parameters, such as the high-frequency viscosity ( $\eta_s$ ), plateau modulus ( $G_p$ ), and relaxation time ( $\lambda$ ), using an appropriate solvent with viscosity  $\eta_s$ , setting optical trap stiffness  $k = 6\pi a G_p$ , and regulating the diffusion profile of the optical trap, respectively, where  $a$  is the Stokes radius of the probe sphere. We validate our scheme by comparing the microrheological response obtained from the probe dynamics in the diffusing optical trap with that of real single-relaxation VE fluids and the theoretical predictions of the HBBP with long-time diffusion model.

**Single-relaxation VE fluids** – We measured the microrheological response of a polystyrene (PS) probe particle ( $2a = 1.98 \mu\text{m}$ ) by recording and analyzing its dynamics in two types of entangled wormlike micellar solutions: cetyltrimethylammonium bromide–sodium salicylate (CTAB–NaSal) and cetylpyridinium bromide–sodium salicylate (CPyBr–NaSal), across various concentrations of surfactants and counterions (Video S1). In all cases, the mean square displacement (MSD) of the probe reveals three distinct regimes (Fig. 1). At short time-lags, the particle undergoes free diffusion, manifesting the high-frequency solvent viscosity  $\eta_s$ . At intermediate time-lags, the MSD reaches a plateau, signifying the elastic confinement imposed by the entangled micellar network. At long time-lags, i.e.,  $\tau > \lambda (= \eta/G_p)$ , the plateau gives way to a diffusive regime corresponding to the slow Maxwell relaxation, where  $\lambda$  and  $\eta$  are the relaxation time and low-frequency viscosity, respectively. These three regimes, namely, short-time free diffusion, an intermediate elastic plateau, and long-time diffusion, constitute the hallmarks of single-relaxation VE fluids. Materi-

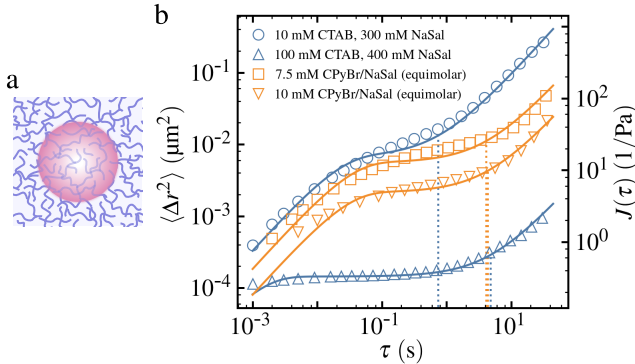


Fig. 1. Typical microrheological response of single-relaxation viscoelastic (VE) fluids. (a) The schematic shows a probe microsphere embedded in a complex fluid represented by entangled wormlike micelles. (b) Microrheological responses of cetyltrimethylammonium bromide–sodium salicylate (CTAB–NaSal) and cetylpyridinium bromide–sodium salicylate (CPyBr–NaSal) are shown at various concentrations, characterized by the MSD ( $\langle \Delta r^2 \rangle$ , left axis) of an embedded  $1.98 \mu\text{m}$  polystyrene (PS) probe particle and derived creep compliance ( $J$ , right axis) using Eq. 5. Open symbols represent the experimentally captured data, and the solid lines of the same color are fits to Eq. 4. The MSDs show three distinct regimes: free diffusion at short time-lags ( $\tau$ ), elastic confinement manifested as plateaus at intermediate  $\tau$ , and diffusive dynamics at  $\tau > \lambda$ , where  $\lambda$  is the relaxation time (marked by vertical dotted lines).

als exhibiting this behavior with a pronounced elastic plateau are well described by the MV fluid model, in which the Voigt and Maxwell elements are connected in series and share a common spring constant  $k$  (Fig. 2a). We fitted the measured MSDs to the theoretical prediction of the HBBP with long-time diffusion model (Fig. 2b), and their excellent agreement validated the MV description of the VE fluids across all concentrations examined.

**HBBP with long-time diffusion model** – The dynamics of a probe particle in an MV fluid can be modeled by that of an HBBP with long-time diffusion (Fig. 2b) [45]. In this model, the probe particle of radius  $a$  diffuses in a solvent of viscosity  $\eta_s$  under harmonic confinement with a spring constant  $k = 6\pi a G_p$ , capturing the Voigt-solid response. The center of this harmonic well (HW) itself undergoes slow Brownian diffusion, incorporating the long-time Maxwell relaxation, which can be regulated by a tunable friction coefficient  $\gamma_{\text{HW}} = 6\pi a \eta_{\text{HW}} = 6\pi a \eta$ , where  $\eta_{\text{HW}}$  is the viscosity associated with the diffusion of the HW, and  $\eta$  is the low-frequency viscosity of the MV fluid. The overdamped Langevin equations representing the probe dynamics consist of two parts: one for the HBBP, describing the position of the probe  $x_{\text{HBBP}}$  relative to the HW center, and the other for the diffusion of the HW center  $x_{\text{HW}}$ . The equations are given by

$$\dot{x}_{\text{HBBP}}(t) = -\frac{x_{\text{HBBP}}(t)}{\tau_k} + v_{r,\text{HBBP}}(t), \quad \text{and} \quad (1a)$$

$$\dot{x}_{\text{HW}}(t) = v_{r,\text{HW}}(t), \quad (1b)$$

where  $\tau_k = \gamma_s/k$  is the equilibration time of the particle, with the drag coefficient  $\gamma_s = 6\pi a \eta_s$ . The terms  $v_{r,\text{HBBP}}(t)$  and  $v_{r,\text{HW}}(t)$  are independent white Gaussian velocity noises with zero mean and correlation  $\langle v_{r,i}(t_1) v_{r,j}(t_2) \rangle = 2D_i \delta_{ij} \delta(t_1 - t_2)$ , where  $D_i$  is the translational diffusivity, and  $i, j \in \{\text{HBBP}, \text{HW}\}$ .

The PDF for the position of HBBP at time  $t$ , denoted by  $p(x_{\text{HBBP}}, t)$ , is described by the Green's function  $G(x_{\text{HBBP}}, t; x_{\text{HBBP}}, 0)$  [46, 47],

$$G(x_{\text{HBBP}}, t; x_{\text{HBBP}}, 0) = [2\pi B(t)]^{-1/2} e^{-(x_{\text{HBBP}} - A(t))^2 / 2B(t)}, \quad (2)$$

where  $A(t) = x_{\text{HBBP},0} e^{-t/\tau_k}$  and  $B(t) = [k_B T/k] (1 - e^{-2t/\tau_k})$ . The PDF of  $x_{\text{HW}}$  is also Gaussian with time-dependent variance  $2D_{\text{HW}} t$ , given by

$$p(x_{\text{HW}}, t) = [2\pi D_{\text{HW}} t]^{-1/2} e^{-(x_{\text{HW}} - x_{\text{HW},0})^2 / 2D_{\text{HW}} t}. \quad (3)$$

The time evolution of these two PDFs,  $p(x_{\text{HBBP}}, t)$  and  $p(x_{\text{HW}}, t)$ , is shown in Fig. 2c.

Because the Maxwell and Voigt elements are connected in series, the particle position in the MV fluid is the sum of the two uncorrelated contributions:  $x(t) = x_{\text{HBBP}}(t) + x_{\text{HW}}(t)$ . Hence, the MSD of a probe particle in an MV fluid can be derived by adding the MSD of the HBBP and that of the HW,

$$\langle \Delta r^2(\tau) \rangle = 4D_{\text{HBBP}} \tau_k \left(1 - e^{-\tau/\tau_k}\right) + 4D_{\text{HW}} \tau. \quad (4)$$

A typical MSD of a probe particle in an MV fluid, modeled as an HBBP with long-time diffusion, is shown in Fig. 2d.

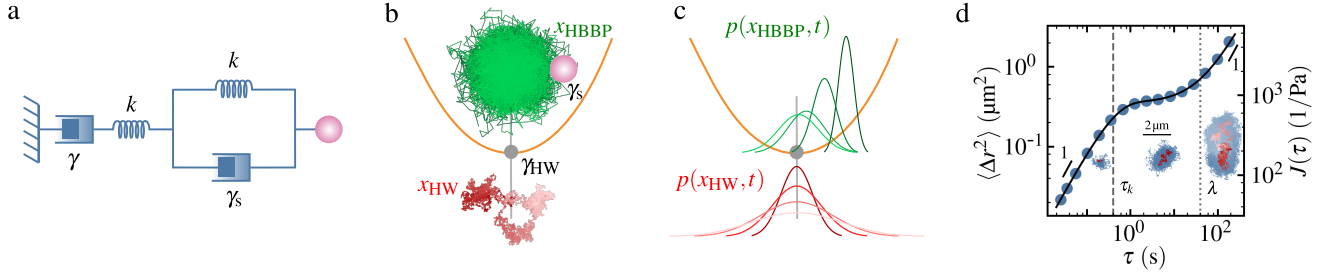


Fig. 2. Harmonically bound Brownian particle (HBBP) with long-time diffusion model describing the microrheological response of an MV fluid. (a) A schematic shows the spring-dashpot model of a Maxwell-Voigt (MV) fluid, constituted by two springs with a common spring constant ( $k = 6\pi a G_p$ ) and dashpots with different damping coefficients ( $\gamma_s$  and  $\gamma$ ) corresponding to the high- and low-frequency viscosities ( $\eta_s$  and  $\eta$ ), respectively. (b) Pictorial illustration of the HBBP with long-time diffusion model exhibits the typical confined dynamics of a HBBP (magenta filled circle) with instantaneous position  $x_{\text{HBBP}}(t)$  (green), and the long-time diffusion of the harmonic well (HW) by a representative trajectory  $x_{\text{HW}}(t)$  (red). The friction coefficient  $\gamma_s$  governs the short-time diffusion of the particle, whereas  $\gamma_{\text{HW}}$ , a tuneable parameter that regulates the long-time diffusion of the HW center, corresponds to  $\gamma$  of the MV model in (a) and the post-relaxation low-frequency viscosity of the MV fluid  $\eta = \gamma_{\text{HW}}/6\pi a$ , which is same as the viscosity associated with the diffusion of the HW,  $\eta_{\text{HW}} = \gamma_{\text{HW}}/6\pi a$ . (c) Time evolution of the position distribution of the HBBP in reference to the HW,  $p(x_{\text{HBBP}}, t)$  (green), and that of the HW in the laboratory frame,  $p(x_{\text{HW}}, t)$  (red), are shown at four progressing times (lighter shades indicate later times). (d) Filled symbols show the simulated MSD ( $\langle \Delta r^2 \rangle$ , left axis) of a  $1.98 \mu\text{m}$  probe sphere in an MV fluid from Langevin dynamics (Eq. 1) and the corresponding creep compliance ( $J$ , right axis), with black line showing fits to the theoretical prediction of the model (Eq. 4). The dashed and dotted vertical lines mark the timescales  $\tau_k$  and  $\lambda$  at which the plateau is reached and the elastic confinement is relaxed, respectively. The blue trajectories represent the probe dynamics at three different times ( $t = \{1, 10, 100\}$  s), with the slowly diffusing HW overlaid in red.

The VE properties of the MV fluid can be extracted from the MSD via GSER,  $\tilde{G}_p(s) = k_B T / \pi a s \langle \Delta \tilde{r}^2(s) \rangle$  where  $\langle \Delta \tilde{r}^2(s) \rangle = \mathcal{L} \{ \Delta r^2(\tau) \}$  [23]. Thus, the creep compliance  $J(\tau)$  is given by

$$J(\tau) = \frac{\pi a}{k_B T} \langle \Delta r^2(\tau) \rangle. \quad (5)$$

This model captures the hallmark features of the microrheological response of single-relaxation VE fluids with a prominent elastic plateau, as observed in entangled wormlike micellar solutions (Fig. 1).

**Extension of the model beyond single-relaxation** – The diffusing trap framework also extends to generalized linear viscoelastic (GLVE) materials with multiple relaxation modes [48]. Each additional noise correlation in the HW dynamics introduces a new elastic plateau at the correlation time, thereby enabling systematic construction of generalized Maxwell models (GMM) through controlled noise superposition. We demonstrate this by introducing a second harmonic component with timescale  $\tau_{k,2}$  in the HW dynamics, creating an effective double-relaxation VE response. The resulting particle MSD is given by

$$\langle \Delta r^2(\tau) \rangle = \sum_{i=1}^2 4D_i \tau_{k,i} \left( 1 - e^{-\tau/\tau_{k,i}} \right). \quad (6)$$

The MSD exhibits two distinct plateaus at times  $\tau_{k,1}$  and  $\tau_{k,2}$ , with the first mode relaxing at finite time  $\lambda_1$  and the second at  $\lambda_2 \rightarrow \infty$ , corresponding to an HBBP whose bounding potential diffuses within a weaker static HW [48].

Active VE environments, such as active entangled polymer networks exhibit persistent motion that fundamentally differs from thermal fluctuations [19, 21, 22]. By imposing persistent

noise on the HW trajectory, we create an effective active VE environment that captures key features of activity-driven systems. In this case, we translate the HW following an active Brownian particle (ABP) trajectory, given by

$$\dot{\mathbf{r}}_{\text{HW}}(t) = V \hat{\phi} + \mathbf{v}_{r,\text{HW}}(t) \quad (7)$$

where  $V$  is the propulsion speed and  $\hat{\phi}$  is the unit vector along the propulsion direction, which is governed by the rotational diffusivity  $D_R$ . The strength of activity is measured by the Péclet number,  $\text{Pe} = V / \sqrt{D_R D_{\text{HW}}}$ , with  $\text{Pe} \gg 1$  indicating that active motion dominates thermal diffusion. This generates persistent motion of the probe particle with a correlation time  $\tau_R = 1/D_R$ .

Therefore, the resulting MSD of the probe particle in this active VE environment is given by

$$\langle \Delta r^2(\tau) \rangle = 4D_{\text{HBBP}} \tau_k \left( 1 - e^{-\tau/\tau_k} \right) + 4D_{\text{HW}} \tau + 2V^2 \tau_R^2 \left( \tau/\tau_R + e^{-\tau/\tau_R} - 1 \right). \quad (8)$$

The particle exhibits free diffusion at short time-lags  $\tau \ll \tau_k$ , manifesting the solvent viscosity. Subsequently, it experiences elastic confinement by the entangled network at  $\tau > \tau_k$ . In the post-relaxation regime ( $\tau > \lambda$ ), the particle exhibits superdiffusive motion for  $\tau < \tau_R$ , transitioning to diffusive dynamics at  $\tau > \tau_R$ . This framework enables systematic investigation of passive probe dynamics in active VE environments across varying activity and viscoelasticity.

**Simulation of probe particle dynamics in an MV fluid** – We simulated the probe particle dynamics in an MV fluid to validate our model for characterizing real single-relaxation VE materials. The numerical simulation was performed in two

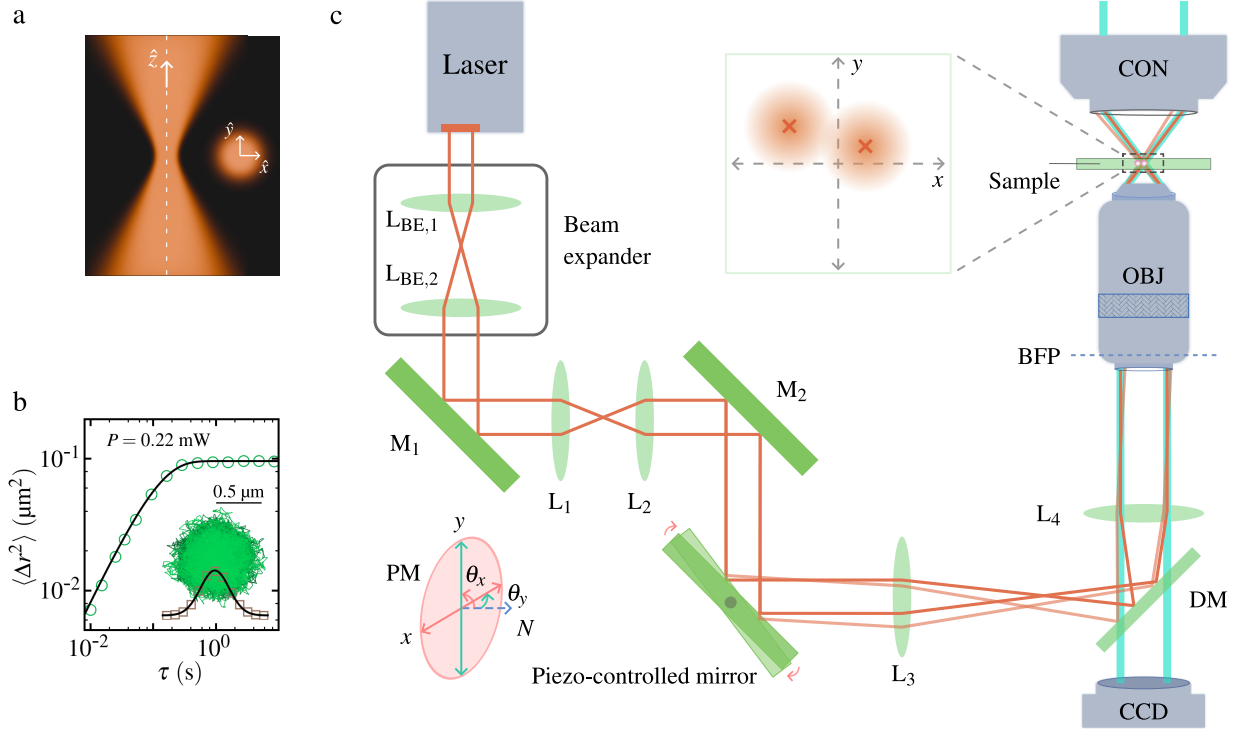


Fig. 3. Experimental realization of the microrheological response of a configurable VE fluid with a dynamic optical trap. (a) The orange gradients show the axial and radial intensity profiles of a tightly focused laser beam propagating along  $\hat{z}$ , creating harmonic confinement at the focal point in the  $x$ - $y$  plane. (b) The MSD ( $\langle \Delta r^2 \rangle$ ) of a  $1.98 \mu\text{m}$  PS probe sphere in a static optical trap exhibits the microrheological response of a Voigt solid, with the corresponding bound trajectory and overlaid long-time position distribution  $p(x_{\text{HBBP}})$  shown in the inset. (c) The ray diagram shows a steerable optical trap. L and M denote the lenses and mirrors in the laser beam path (orange lines). The trap is steered in the focal ( $x$ - $y$ ) plane by regulating the tilt ( $\theta_x$ ,  $\theta_y$ ) of the piezo-controlled mirror, which is placed at the conjugate image plane of the back focal plane (BFP) of the objective, following Eq. 9. CON, OBJ, DM, and CCD in the illumination beam path (cyan lines) denote condenser, objective, dichroic mirror, which reflects the trapping laser and transmits the illumination, and a CCD camera, respectively. The bottom left inset illustrates the tilt angles  $\theta_x$  and  $\theta_y$  around the  $x$ - and  $y$ -axis of the mirror mount. The top inset shows the resultant displacement of the trap (orange gradient) at the focal plane.

steps: first, we computed the position of the particle in the HW using Green's function, as  $x_{\text{HBBP}}(t_n) = x_{\text{HBBP}}(t_{n-1})e^{-\Delta t/\tau_k} + \sqrt{B(\Delta t)}R_{\text{HBBP}}(t_n)$ , and second, obtained the HW center position from a simple diffusion process as  $x_{\text{HW}}(t_n) = x_{\text{HW}}(t_{n-1}) + \sqrt{2D_{\text{HW}}\Delta t}R_{\text{HW}}(t_n)$ , where both  $R_{\text{HBBP}}(t_n)$  and  $R_{\text{HW}}(t_n)$  are Gaussian random numbers with zero mean and unit standard deviation. By updating the initial HBBP position at every step ( $n$ ), we obtained the particle position as  $x(t_n) = x_{\text{HBBP}}(t_n) + x_{\text{HW}}(t_n)$  [45, 48]. The resulting  $\langle \Delta r^2 \rangle$  and creep compliance  $J(\tau)$  were computed from the simulated trajectories, as shown in Fig. 2d. At short time-lags, the probe particle exhibits diffusive dynamics and experiences harmonic confinement at the equilibration time  $\tau_k$ , leading to a plateau in the MSD. As the system relaxes at  $\tau > \lambda (= \tau_k(D_{\text{HBBP}}/D_{\text{HW}}))$  due to the slow diffusion of the HW, the probe particle dynamics become diffusive again with a smaller diffusion coefficient corresponding to  $D_{\text{HW}}$ . These results show excellent agreement with the experimentally observed microrheological response of single-relaxation VE fluids (Fig. 1b).

**Experimental realization of configurable VE environments** – We trapped a dielectric PS particle ( $2a = 1.98 \mu\text{m}$ ) in an HW

created by a conventional optical tweezers setup with a linearly polarized solid-state continuous wave Nd:YAG laser at  $\lambda = 1064 \text{ nm}$  operating in  $\text{TEM}_{00}$  Gaussian mode, as shown in Fig. 3a (model: Laser Quantum Opus 5 W), focused through a  $60\times$  oil-immersion microscope objective with NA 1.40 (model: Nikon CFI Plan APO Lambda) [49, 50]. The trapped particle underwent confined Brownian motion in the HW centered at the laser focal point, with the measured MSD and position distribution corroborating the HBBP dynamics and manifesting the microrheological response of a Voigt solid (Fig. 3b). Our setup incorporates a piezo-controlled steering mirror placed at the conjugate image plane of the back focal plane of the microscope objective. We implemented this using an afocal lens pair  $L_3$  and  $L_4$  (Fig. 3c), which ensured that the angular displacement of the mirror translated to lateral displacement of the optical trap in the focal plane [49–51]. This configuration enables any predefined  $x$ - $y$  movement of the optical trap (Fig. 3c (top inset)) by controlling the tilt  $\theta_x$ ,  $\theta_y$  of the steering mirror (Fig. 3c (bottom left inset)).

The piezo-mirror tilt  $\Delta\theta_{\text{PM}}$  produces an angular displacement  $\Delta\theta_{\text{BFP}}$  at the back focal plane of the objective and a

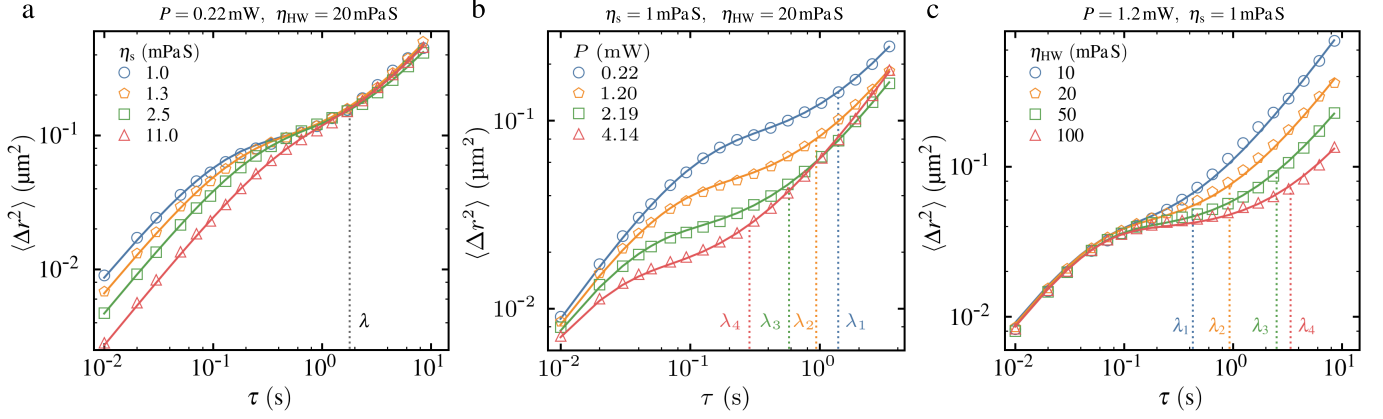


Fig. 4. Systematic experimental tuning of the VE parameters in the microrheological response of a configurable single-relaxation VE environment. The response is exhibited by the MSD of a 1.98  $\mu\text{m}$  diameter PS probe particle in a diffusive optical trap. The experimental data are shown with open symbols, whereas the solid lines of the same color represent the corresponding theoretical predictions of our model (Eq. 4). (a) Systematic variation of the high-frequency viscosity  $\eta_s$  of the emergent VE environment is achieved by using viscous media of different viscosities. Here,  $\eta_s$  is varied while keeping  $G_p$  and  $\lambda$  unchanged, as the trap stiffness  $k = 6\pi a G_p$  ( $\propto$  laser power  $P$ ) and the viscosity of the diffusing trap  $\eta_{\text{HW}}$  remain constant. (b) The plateau modulus  $G_p$  is regulated by varying the laser power  $P$  while keeping  $\eta_s$  and  $\eta_{\text{HW}}$  unchanged. An increase in  $G_p$  diminishes the MSD plateau value and shifts both  $\tau_k = \eta_s/G_p$  and  $\lambda = \eta_{\text{HW}}/G_p$  to shorter time-lags. (c) Independent variation of  $\lambda$  is achieved by varying  $\eta_{\text{HW}}$ , i.e.,  $\eta_{\text{HW}}$ , while keeping  $G_p$  and  $\eta_s$  unchanged. The MSDs show identical short-time diffusion but systematically different relaxation times.

corresponding lateral displacement  $\Delta r$  in the focal plane, given by

$$\Delta\theta_{\text{BFP}} = -2\frac{f_3}{f_4}\Delta\theta_{\text{PM}}, \quad \Delta r = f_{\text{EFL}}\Delta\theta_{\text{BFP}}, \quad (9)$$

where  $f_3$  and  $f_4$  are the focal lengths of lenses  $L_3$  and  $L_4$ , respectively, and  $f_{\text{EFL}}$  is the effective focal length of the objective. We generated an angular displacement time series  $(\Delta\theta_x(t), \Delta\theta_y(t))$  for the steering mirror, corresponding to the required diffusion profile  $(\Delta x(t), \Delta y(t))$  of the HW, and fed it to the piezo-controller. This realizes the appropriate HW dynamics for a desired relaxation behavior of the configurable VE environment.

To examine the precise and reliable movement of the HW, we tightly confined a particle using high laser power, reducing its thermal fluctuations within the trap. In this setting, the particle position closely follows the HW center. We moved the trap along a predefined Brownian trajectory by feeding the corresponding angular displacement time series to the piezo-controller and recorded the particle dynamics using a CCD camera. The particle position was tracked using the Track-Mate plugin in ImageJ [52], and the obtained trajectory closely followed the programmed trap trajectory (Video S2a).

The MV model describes the VE response of single-relaxation complex fluids using three parameters: high-frequency viscosity  $\eta_s$ , plateau modulus  $G_p$ , and relaxation time  $\lambda$ . Here, we employed a dynamic optical trap to directly regulate these three parameters in the response of a trapped particle, constructing a configurable VE environment where  $\eta_s$ ,  $G_p$ , and  $\lambda$  can be tuned systematically.

*Tuning high-frequency viscosity  $\eta_s$*  – The high-frequency viscosity  $\eta_s$  of a VE medium governs the probe particle dynamics at short time-lags, before elastic confinement sets in and the

MSD reaches a plateau at the characteristic time  $\tau_k = \eta_s/G_p$ . Moreover,  $\eta_s$  directly regulates  $\tau_k$ , as they are linearly related at fixed  $G_p$ . We tuned  $\eta_s$  by choosing an appropriate viscous medium, using aqueous dilutions of glycerol with concentrations from 10 to 60 wt% at 22  $^\circ\text{C}$  to vary  $\eta_s$  from 1.3 to 11 mPaS, well beyond pure water (1 mPaS) [53]. With increasing  $\eta_s$ , the diffusivity of the probe particle decreases and the MSDs shift downward. Hence, the plateau in the MSD is reached at longer time-lags, resulting in a longer  $\tau_k$  when  $G_p$  and  $\lambda$  remain unchanged. The effect of independently varying  $\eta_s$  on the MSD of a probe particle is demonstrated in Fig. 4a (Video S2b).

*Tuning plateau modulus  $G_p$*  – The plateau modulus  $G_p$ , determined from the plateau value of the MSD, corresponds directly to the elastic modulus of a Voigt solid. In our configurable VE environment,  $G_p$  is directly controlled by the laser power  $P$ , as the trap stiffness  $k$  varies proportionally with  $P$ , following  $G_p = k/6\pi a$ . Moreover, an increase in  $G_p$  shifts both the crossover time  $\tau_k = \eta_s/G_p$  and the relaxation time  $\lambda = \eta_{\text{HW}}/6\pi a G_p = \eta_{\text{HW}}/G_p$  to shorter time-lags, reducing and expanding the high- and low-frequency diffusive behaviors, respectively. This coupled response of  $\tau_k$  and  $\lambda$  through  $G_p$  is a hallmark property of real single-relaxation VE materials, where increasing elasticity shortens both timescales. The independent and systematic tuning of the plateau modulus  $G_p$  through the laser power  $P$  is shown in Fig. 4b (Video S2c).

*Tuning relaxation time  $\lambda$*  – The relaxation time  $\lambda$  defines the timescale at which the residual stress equilibrates and the elastic response of the VE medium decays, beyond which the medium behaves like a viscous fluid. In our configurable VE environment,  $\lambda$  can be independently tuned by varying the viscosity  $\eta_{\text{HW}}$  associated with the imposed diffusive motion of the optical trap, keeping  $G_p$  and  $\eta_s$  con-

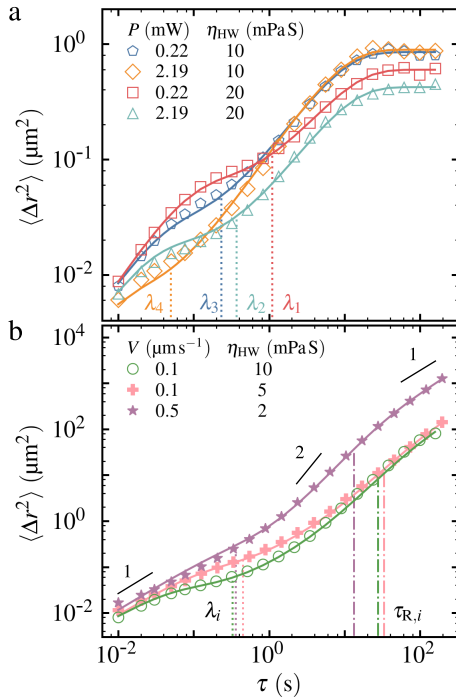


Fig. 5. Realization of double-relaxation VE media and active VE environments employing a dynamic trap scheme. The MSDs of a 1.98  $\mu\text{m}$  diameter PS probe particle in a dynamic trap with correlated and persistent translational noise, exhibiting microrheological response of configurable double-relaxation and active VE environments. The experimental data and simulation results are shown with open and filled symbols, respectively, whereas the solid lines of the same color represent the corresponding theoretical predictions. All relevant parameters are given in the insets. (a) Microrheological response of double-relaxation VE environments is generated by translating the trap with exponentially correlated noise, providing equilibration timescales  $\tau_{k,1}$  and  $\tau_{k,2}$ . The MSDs exhibit two distinct plateaus separated by an intermediate relaxation, demonstrating hierarchical VE response consistent with Eq. 6 (solid line). (b) Probe particle dynamics in active VE baths is realized by moving the trap along an ABP trajectory with persistent translational noise. The MSDs exhibit features similar to those of probe particles in a single-relaxation VE fluid, with distinct post-relaxation ( $\tau > \lambda$ ) behavior showing super-diffusive and diffusive dynamics before and after the persistence time  $\tau_R$ , respectively, as predicted by Eq. 8.

stant. The relaxation time  $\lambda$  and the low-frequency viscosity  $\eta = \gamma_{\text{HW}}/6\pi a = \eta_{\text{HW}}$  are coupled through the plateau modulus  $G_p$  as  $\lambda = \gamma_{\text{HW}}/6\pi a G_p = \eta_{\text{HW}}/G_p$ . At fixed  $G_p$ , i.e., at a constant laser power, systematic regulation of the relaxation time  $\lambda$  and, consequently, the low-frequency viscosity was realized by choosing an appropriate  $\eta_{\text{HW}}$  for the trap movement. With increasing  $\lambda$ , the system relaxes more slowly and the long-time diffusive behavior in the MSD shifts to longer time-lags. The independent variation of  $\lambda$  by regulating  $\eta_{\text{HW}}$  is illustrated in Fig. 4c (Video S2d).

**Double-relaxation VE media** – Our scheme is extendable to realize the microrheological response of VE media with double relaxation. Here, we demonstrate this by showing the MSD of a probe particle in a diffusing optical trap that follows

a trajectory with exponentially correlated noise (Video S3a). This yields a longer equilibration timescale  $\tau_{k,2}$ , corresponding to the correlation time of the imposed noise, in addition to the shorter equilibration time  $\tau_{k,1}$  associated with the stiffness of the optical trap. Thereby, both equilibration timescales, and hence the two plateaus in the MSD, can be independently configured by regulating the trap stiffness through the laser power  $P$  and the correlation time of the imposed noise in the trap dynamics. Fig. 5a shows the experimentally measured MSD of a 1.98  $\mu\text{m}$  PS particle (open symbols) displaying two distinct plateaus separated by an intermediate relaxation regime, consistent with the hierarchical VE response predicted by Eq. 6 (solid line). This signifies that multiple plateaus in the MSD can be systematically configured using an appropriate noise profile with multiple correlation timescales. Therefore, our results demonstrate that this dynamic trap framework extends beyond replicating the microrheological response of single-relaxation MV fluids and can emulate that of a broad class of VE media following the GMM with a relaxation spectrum [48].

**Active VE environments** – Our approach can also generate probe particle dynamics in an active VE environment, such as an entangled network of active polymers [18–22], by moving the trap along an ABP trajectory with persistent noise. Fig. 5b shows the experimentally obtained MSD of a 1.98  $\mu\text{m}$  PS particle manifesting post-relaxation active dynamics (Video S3b), as predicted by Eq. 8. At short time-lags  $\tau < \lambda$ , before relaxation, the microrheological response is similar to that of a Voigt solid, exhibiting a diffusive regime at  $\tau \ll \tau_k$  with a subsequent plateau arising from elastic confinement. At  $\tau > \lambda$ , the active persistent motion of the trap induces super-diffusive dynamics of the probe particle with an exponent of  $\sim 2$ . The probe dynamics become diffusive again at  $\tau > \tau_R$  as the correlation of the propulsion direction, or equivalently the persistence in the translational noise, decays. The experimentally observed MSD (open symbols) shows excellent agreement with those from numerical simulations (filled symbols) and theoretical predictions (Eq. 8, solid line). These results demonstrate that our dynamic trap scheme provides a convenient route for studying probe particle dynamics and microrheological response of active VE environments, where the activity and VE properties can be independently and systematically regulated.

**Conclusions** – In this study, we demonstrate a novel experimental scheme for realizing the microrheological response of an emergent configurable VE environment by appropriately regulating the stiffness and trajectory of the dynamic optical trap. While the stiffness of the optical trap regulates the plateau modulus  $G_p$  of the VE fluid, the relaxation time  $\lambda$  and post-relaxation properties are governed by the trap dynamics. Thereby, our approach enables systematic and independent variation of the VE properties of the resultant system, overcoming the inherent coupling in real complex fluids. The microrheological measurements from the emergent configurable VE environment exhibit quantitative similarities with those from real complex fluids, having widely varied VE properties, validating the broad applicability of our scheme.

The key advantage of this approach lies in its experimental versatility: the systematic variation of the stiffness and

dynamics of an optical trap enables the rapid exploration of VE parameter space. Furthermore, it provides access to VE regimes that are challenging to achieve with real complex fluids and remain mostly unaltered against variations in experimental settings, such as the temperature and surface chemistry of the probe particles. The framework extends naturally to replicate the microrheological response of GLVE materials having multiple relaxation spectra with correlated noise in the dynamics of the trap and to active VE environments by translating the trap along an ABP trajectory.

Notably, this approach with a single dynamic optical trap cannot capture nonlinear VE responses observed in various active microrheology measurements, such as strain-stiffening, shear-thinning, strain-induced density inhomogeneities and recoil [54–56]. However, this limitation can be overcome in future studies by using an array of weak traps that replicate the adjoining confinement in an entangled network. Beyond passive systems, our scheme enables the study of probe par-

ticle dynamics in configurable active VE environments. The experimental scheme reported in this study opens diverse future directions for investigating the dynamics of natural and artificial microswimmers in controlled VE environments and the VE properties of entangled active biopolymers.

**Acknowledgements** – Research funding from SERB (now ANRF), Govt. of India (Grant No. CRG/2020/002723) is gratefully acknowledged. M.K. acknowledges funding from IIT Kanpur through an initiation grant (grant no. IITK-PHY-2017081).

**Disclosures** – The authors declare no competing interest.

**Data availability** – All data required to reach the conclusions of this study are presented in the manuscript.

**Author contributions** – All authors contributed to the conception and design of the research. S.H. conducted the experiments and analyzed the data. S.H. and M.K. interpreted the data and wrote the manuscript. M.K. supervised the project.

## References –

- [1] T. Shikata, H. Hirata, E. Takatori, and K. Osaki, Nonlinear viscoelastic behavior of aqueous detergent solutions, *Journal of Non-Newtonian Fluid Mechanics* **28**, 171 (1988).
- [2] M. E. Cates and S. J. Candau, Statics and dynamics of worm-like surfactant micelles, *J. Phys.: Condens. Matter* **2**, 6869 (1990).
- [3] F. Kern, P. Lemarechal, S. J. Candau, and M. E. Cates, Rheological properties of semidilute and concentrated aqueous solutions of cetyltrimethylammonium bromide in the presence of potassium bromide, *Langmuir* **8**, 437 (1992).
- [4] M. Bellour, M. Skouri, J.-P. Munch, and P. Hébraud, Brownian motion of particles embedded in a solution of giant micelles, *Eur. Phys. J. E* **8**, 431 (2002).
- [5] F. Cardinaux, L. Cipelletti, F. Scheffold, and P. Schurtenberger, Microrheology of giant-micelle solutions, *Europhys. Lett.* **57**, 738 (2002).
- [6] P. A. Hassan, K. Bhattacharya, S. K. Kulshreshtha, and S. R. Raghavan, Microrheology of Wormlike Micellar Fluids from the Diffusion of Colloidal Probes, *J. Phys. Chem. B* **109**, 8744 (2005).
- [7] T. G. Mason, H. Gang, and D. A. Weitz, Diffusing-wave-spectroscopy measurements of viscoelasticity of complex fluids, *J. Opt. Soc. Am. A* **14**, 139 (1997).
- [8] J. D. Ferry, *Viscoelastic Properties of Polymers*, 3rd ed. (Wiley, New York, 1980).
- [9] M. E. Cates, Reptation of living polymers: Dynamics of entangled polymers in the presence of reversible chain-scission reactions, *Macromolecules* **20**, 2289 (1987).
- [10] T. G. Mason, K. Ganesan, J. H. Van Zanten, D. Wirtz, and S. C. Kuo, Particle Tracking Microrheology of Complex Fluids, *Phys. Rev. Lett.* **79**, 3282 (1997).
- [11] B. R. Dasgupta, S.-Y. Tee, J. C. Crocker, B. J. Frisken, and D. A. Weitz, Microrheology of polyethylene oxide using diffusing wave spectroscopy and single scattering, *Phys. Rev. E* **65**, 051505 (2002).
- [12] Z. Cheng and T. G. Mason, Rotational Diffusion Microrheology, *Phys. Rev. Lett.* **90**, 018304 (2003).
- [13] J. H. Van Zanten, S. Amin, and A. A. Abdala, Brownian Motion of Colloidal Spheres in Aqueous PEO Solutions, *Macromolecules* **37**, 3874 (2004).
- [14] E. Andablo-Reyes, P. Díaz-Leyva, and J. L. Arauz-Lara, Microrheology from Rotational Diffusion of Colloidal Particles, *Phys. Rev. Lett.* **94**, 106001 (2005).
- [15] M. L. Gardel, M. T. Valentine, J. C. Crocker, A. R. Bausch, and D. A. Weitz, Microrheology of Entangled F-Actin Solutions, *Phys. Rev. Lett.* **91**, 158302 (2003).
- [16] J. N. Wilking and T. G. Mason, Optically driven nonlinear microrheology of gelatin, *Phys. Rev. E* **77**, 055101 (2008).
- [17] S. Shabaniverki and J. J. Juárez, Characterizing gelatin hydrogel viscoelasticity with diffusing colloidal probe microscopy, *Journal of Colloid and Interface Science* **497**, 73 (2017).
- [18] D. Mizuno, C. Tardin, C. F. Schmidt, and F. C. MacKintosh, Nonequilibrium Mechanics of Active Cytoskeletal Networks, *Science* **315**, 370 (2007).
- [19] T. Eisenstecken, G. Gompper, and R. G. Winkler, Internal dynamics of semiflexible polymers with active noise, *The Journal of Chemical Physics* **146**, 154903 (2017).
- [20] A. R. Tejedor and J. Ramírez, Reptation of Active Entangled Polymers, *Macromolecules* **52**, 8788 (2019).
- [21] R. G. Winkler and G. Gompper, The physics of active polymers and filaments, *The Journal of Chemical Physics* **153**, 040901 (2020).
- [22] A. R. Tejedor, R. Carracedo, and J. Ramírez, Molecular dynamics simulations of active entangled polymers reptating through a passive mesh, *Polymer* **268**, 125677 (2023).
- [23] T. M. Squires and T. G. Mason, Fluid Mechanics of Microrheology, *Annu. Rev. Fluid Mech.* **42**, 413 (2010).
- [24] T. Mason, H. Gang, and D. Weitz, Rheology of complex fluids measured by dynamic light scattering, *Journal of Molecular Structure* **383**, 81 (1996).
- [25] T. G. Mason and D. A. Weitz, Optical Measurements of Frequency-Dependent Linear Viscoelastic Moduli of Complex Fluids, *Phys. Rev. Lett.* **74**, 1250 (1995).
- [26] F. Gittes, B. Schnurr, P. D. Olmsted, F. C. MacKintosh, and C. F. Schmidt, Microscopic Viscoelasticity: Shear Moduli of Soft

- Materials Determined from Thermal Fluctuations, *Phys. Rev. Lett.* **79**, 3286 (1997).
- [27] T. G. Mason, Estimating the viscoelastic moduli of complex fluids using the generalized Stokes–Einstein equation, *Rheologica acta* **39**, 371 (2000).
- [28] J. C. Crocker, M. T. Valentine, E. R. Weeks, T. Gisler, P. D. Kaplan, A. G. Yodh, and D. A. Weitz, Two-Point Microrheology of Inhomogeneous Soft Materials, *Phys. Rev. Lett.* **85**, 888 (2000).
- [29] E. M. Furst and T. M. Squires, *Microrheology*, first published in paperback ed. (Oxford University Press, Oxford, 2020).
- [30] Yu. L. Raikher and V. V. Rusakov, Theory of Brownian motion in a Jeffreys fluid, *J. Exp. Theor. Phys.* **111**, 883 (2010).
- [31] Y. L. Raikher, V. V. Rusakov, and R. Perzynski, Brownian motion in a viscoelastic medium modelled by a Jeffreys fluid, *Soft Matter* **9**, 10857 (2013).
- [32] J. H. Van Zanten and K. P. Rufener, Brownian motion in a single relaxation time Maxwell fluid, *Phys. Rev. E* **62**, 5389 (2000).
- [33] C. Wilhelm, F. Gazeau, and J.-C. Bacri, Rotational magnetic endosome microrheology: Viscoelastic architecture inside living cells, *Phys. Rev. E* **67**, 061908 (2003).
- [34] C. Wilhelm and F. Gazeau, Magnetic nanoparticles: Internal probes and heaters within living cells, *Journal of Magnetism and Magnetic Materials* **321**, 671 (2009).
- [35] M. Grimm, S. Jeney, and T. Franosch, Brownian motion in a Maxwell fluid, *Soft Matter* **7**, 2076 (2011).
- [36] V. V. Rusakov, Yu. L. Raikher, and R. Perzynski, Brownian Motion in the Fluids with Complex Rheology, *Math. Model. Nat. Phenom.* **10**, 1 (2015).
- [37] A. W. C. Lau, B. D. Hoffman, A. Davies, J. C. Crocker, and T. C. Lubensky, Microrheology, Stress Fluctuations, and Active Behavior of Living Cells, *Phys. Rev. Lett.* **91**, 198101 (2003).
- [38] J. P. Celli, B. S. Turner, N. H. Afdhal, S. Keates, I. Ghiran, C. P. Kelly, R. H. Ewoldt, G. H. McKinley, P. So, S. Erramilli, and R. Bansil, *Helicobacter Pylori* moves through mucus by reducing mucin viscoelasticity, *Proc. Natl. Acad. Sci. U.S.A.* **106**, 14321 (2009).
- [39] A. E. Patteson, A. Gopinath, M. Goulian, and P. E. Arratia, Running and tumbling with *E. coli* in polymeric solutions, *Sci Rep* **5**, 10.1038/srep15761 (2015).
- [40] J. R. Gomez-Solano, A. Blokhuis, and C. Bechinger, Dynamics of Self-Propelled Janus Particles in Viscoelastic Fluids, *Phys. Rev. Lett.* **116**, 10.1103/physrevlett.116.138301 (2016).
- [41] M. Doi and S. F. Edwards, *The Theory of Polymer Dynamics*, reprint ed., International Series of Monographs on Physics No. 73 (Clarendon Press, Oxford, 2013).
- [42] T. M. Squires, Nonlinear Microrheology: Bulk Stresses versus Direct Interactions, *Langmuir* **24**, 1147 (2008).
- [43] Q. Lu and M. J. Solomon, Probe size effects on the microrheology of associating polymer solutions, *Phys. Rev. E* **66**, 061504 (2002).
- [44] J. L. McGrath, J. H. Hartwig, and S. C. Kuo, The Mechanics of F-Actin Microenvironments Depend on the Chemistry of Probing Surfaces, *Biophysical Journal* **79**, 3258 (2000).
- [45] M. Khan and T. G. Mason, Random walks of colloidal probes in viscoelastic materials, *Phys. Rev. E* **89**, 042309 (2014).
- [46] S. Chandrasekhar, Stochastic Problems in Physics and Astronomy, *Rev. Mod. Phys.* **15**, 1 (1943).
- [47] G. E. Uhlenbeck and L. S. Ornstein, On the Theory of the Brownian Motion, *Phys. Rev.* **36**, 823 (1930).
- [48] M. Khan and T. G. Mason, Trajectories of probe spheres in generalized linear viscoelastic complex fluids, *Soft Matter* **10**, 9073 (2014).
- [49] M. Khan, *Optical Tweezers Methods and Applications in Contemporary Research* (Scholars' Press, 2014).
- [50] S. Halder, D. Chanda, D. Mondal, S. Kundu, and M. Khan, Optical Micromanipulation of Soft Materials: Applications in Devices and Technologies, in *Advanced Structured Materials* (Springer Nature Singapore, Singapore, 2024) pp. 415–469.
- [51] E. Fällman and O. Axner, Design for fully steerable dual-trap optical tweezers, *Appl. Opt.* **36**, 2107 (1997).
- [52] D. Ershov, M.-S. Phan, J. W. Pylvänäinen, S. U. Rigaud, L. Le Blanc, A. Charles-Orszag, J. R. W. Conway, R. F. Laine, N. H. Roy, D. Bonazzi, G. Duménil, G. Jacquemet, and J.-Y. Tinevez, TrackMate 7: Integrating state-of-the-art segmentation algorithms into tracking pipelines, *Nat Methods* **19**, 829 (2022).
- [53] J. B. Segur and H. E. Oberstar, Viscosity of Glycerol and Its Aqueous Solutions, *Ind. Eng. Chem.* **43**, 2117 (1951).
- [54] J. R. Gomez-Solano and C. Bechinger, Transient dynamics of a colloidal particle driven through a viscoelastic fluid, *New J. Phys.* **17**, 103032 (2015).
- [55] M. Khan, K. Regan, and R. M. Robertson-Anderson, Optical Tweezers Microrheology Maps the Dynamics of Strain-Induced Local Inhomogeneities in Entangled Polymers, *Phys. Rev. Lett.* **123**, 038001 (2019).
- [56] F. Ginot, J. Caspers, L. F. Reinalter, K. Krishna Kumar, M. Krüger, and C. Bechinger, Recoil experiments determine the eigenmodes of viscoelastic fluids, *New J. Phys.* **24**, 123013 (2022).